ACS APPLIED MATERIALS & INTERFACES

Research Article

www.acsami.org

# In Situ Assembly of Antifouling/Bacterial Silver Nanoparticle-Hydrogel Composites with Controlled Particle Release and Matrix Softening

Kwanghyun Baek,[†] Jing Liang,[‡] Wan Ting Lim,[‡] Huimin Zhao,[‡,§] Dong Hyun Kim,*[,∥] and Hyunjoon Kong*[,‡,§]

[†]Department of Materials Science and Engineering, [‡]Department of Chemical and Biomolecular Engineering, and [§]Carl R. Woese Institute for Genomic Biology, University of Illinois at Urbana−Champaign, Urbana, Illinois 61801, United States

[∥]Department of Human and Culture Convergence Technology R&BD Group, Korea Institute of Industrial Technology, Ansan-si Gyeonggi-do 426-910, South Korea

Supporting Information

**ABSTRACT:** Controlling bacterial contamination has been a major challenge for protecting human health and welfare. In this context, hydrogels loaded with silver nanoparticles have been used to prevent biofilm formation on substrates of interest. However, such gel composites are often plagued by rapid loss of silver nanoparticles and matrix softening, and thus the gel becomes less effective for antifouling. To this end, this study demonstrates that in situ photoreaction of an aqueous mixture of silver nitrates, poly(ethylene glycol) diacrylate, and vinylpyrrolidone results in a silver nanoparticle-laden hydrogel composite with minimal nanoparticle loss and matrix softening due to enhanced binding between nanoparticles and the gel. The resulting gel composite successfully inhibits the bacterial growth in media and the bacterial adhesion to surfaces of interest. We suggest that the results of this study serve to advance quality of materials with antifouling/bacterial activities.

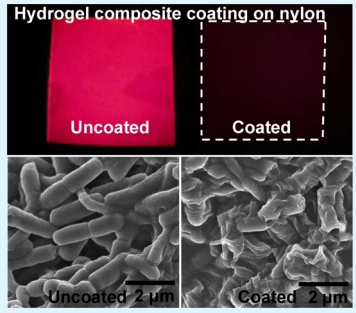


**KEYWORDS:** *hydrogels, silver nanoparticles, biofilm, antibacterial, antifouling*

## 1. INTRODUCTION

Bacterial contamination characterized by uncontrolled microbial growth in water and also on various industrial, household, and biomedical products negatively impacts efforts to protect human health and welfare.[1−6] Because metallic ions dissolved from nanoparticles with a high surface-area-to-mass ratio can damage bacterial cell membrane and also limit cell growth, they have been extensively studied as a way to control the bacterial contamination.[7−13] These metallic nanoparticles are often immobilized in a hydrogel, such that the resulting hydrogel composite can sustainably release metallic ions and subsequently control bacterial cell adhesion and growth over an extended time period.[14−18] These nanoparticles are typically loaded into a preformed hydrogel via infiltration.[19,20] Alternatively, metal ionic precursors are infiltrated into a premade hydrogel, followed by activating reduction to form metallic nanoparticles in the hydrogel.[21,22] Another method involves mixing gel-forming polymers with preformed nanoparticles that are then cross-linked to assemble a gel composite.[23]

The resulting composites demonstrated impressively enhanced antibacterial properties compared with free nanoparticles suspended in aqueous media or blank hydrogels. However, nanoparticles often rapidly diffuse out of the gel matrix, partly because of the absence of association between nanoparticles and hydrogel matrix.[24] Such uncontrolled particle loss from the gel necessitates loading of a large amount of nanoparticles to attain desired performance, thus raising concerns about health and environmental impacts of nanoparticles as well as increasing material costs. The increased loading of preformed nanoparticles also reduces the cross-linking density of the gel, leading to significant decreases in mechanical stiffness and strength of the composite.

To resolve these challenges, we hypothesized that simultaneous photoactivated synthesis of antibacterial nanoparticles and cross-linking of nanoparticle-binding polymers would create a hydrogel composite with enhanced nanoparticle retention and minimal matrix softening. We also proposed that the resulting AgNP-laden gel composite would present improved antifouling and antibacterial properties and would require a smaller amount of particle loading than that conventionally used. We examined this hypothesis by exposing a mixture of poly(ethylene glycol) diacrylate (PEGDA), vinylpyrolidone (VP), and metallic salt solutions including silver nitrate to ultraviolet (UV) lights. The poly(vinylpyrolidone) (PVP) is known to bind with silver nanoparticles via the coordination interaction, while PEGDA allows us to control mechanical stiffness of the gel composite with its concentration.[25,26] A photoinitiator activated by UV light is capable of simultaneously activating radical reduction of metal

Received: April 16, 2015
Accepted: June 5, 2015
Published: June 5, 2015





DOI: 10.1021/acsami.5b03313
ACS Appl. Mater. Interfaces 2015, 7, 15359−15367

ions and cross-linking reaction of the PEGDA and VP. The nanoparticles formed in a gel were examined microscopically and spectroscopically while monitoring mechanical properties of the gel in parallel. Finally, we evaluated the extent to which the gel composite controls bacterial growth in broth media suspended with the gel composites and also biofilm formation on the gel. We further used the gel to coat polymeric/metallic substrates, in order to demonstrate usefulness of the gel as an antifouling/bacterial coating material.

## 2. RESULTS AND DISCUSSION

**In Situ Fabrication of Metallic Nanoparticle-Laden Hydrogel Composites.** Exposing the PEGDA solution mixed with silver nitrates to UV light resulted in hydrogels loaded with silver nanoparticles in situ, as demonstrated by color changes of the hydrogels and transmission electron microscopy images of the nanoparticles (Figure 1a–d). The average diameter of AgNP

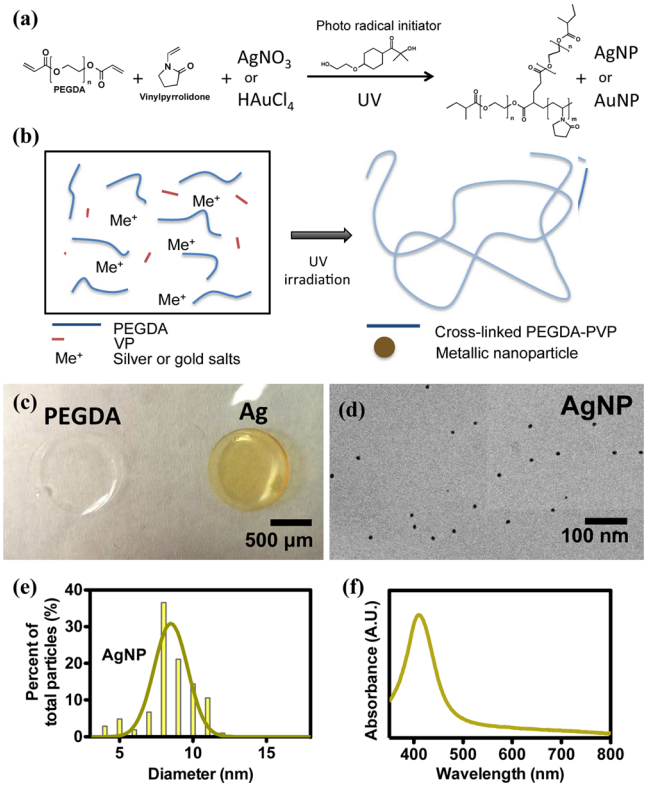


**Figure 1.** In situ assembly of AgNP-hydrogel composites. (a) Chemical reaction scheme of the photoactivated reduction of metallic salts and cross-linking of PEGDA-PVP. (b) Scheme depicting microstructural changes of the pre-gelled mixture to a nanoparticle-laden hydrogel composite. (c) Optical image of AgNP-hydrogel composites. 0.2 mM of silver nitrates was mixed with the pre-gel solution to form the hydrogel composites. (d) TEM image of the hydrogel composites laden with AgNP formed via in situ assembly. (e) Size distribution of AgNP formed in the hydrogel composites. Size was analyzed using TEM images. (f) UV/vis absorption spectra of AgNP formed in the hydrogel matrix.

created in the hydrogel was approximately 8.5 ± 1.1 nm (Figure 1d,e). AgNP formed in the gel presented a face-centered cubic crystal structure with a lattice constant of 4.1 Å, as characterized by selective area diffraction patterns (Figure S1).

The resulting AgNP-hydrogel composite displayed the absorption in a visible area at the wavelengths of 420 and 530 nm, respectively (Figure 1f). Such surface plasmon resonance absorption was similar to that of the nanoparticles formed via conventional reduction of metal ions in aqueous media.[27,28] These nanoparticles remained stable in a gel over a month without any aggregation or precipitation. In contrast, nanoparticles prepared in the aqueous media aggregated within a few days, despite the presence of citrate-based capping molecules on the nanoparticle surface (Figure S2).

The number of nanoparticles formed in the PEGDA hydrogel was further controlled with the irradiation time. The height of the absorption peak at 420 nm was measured to estimate the concentration of nanoparticles formed in a hydrogel following the principal of Beer–Lambert law

$$A = -\log_{10}\frac{I}{I_0} = \varepsilon l c \tag{1}$$

where $A$ represents absorbance; $I_0$ and $I$ are the light intensity before and after passage through the gel, $\varepsilon$ is molar absorptivity, $l$ is thickness of the gel through which the light passes, and $c$ is concentration of nanoparticles.[29] At a given silver nitrate concentration, the absorption peak at 420 nm was increased with the irradiation time, specifically between 5 and 12 min (Figure 2a-1). Furthermore, the number of cross-links for the PEGDA hydrogel was also increased with irradiation time, as demonstrated by the increase of UV absorbance below 400 nm wavelength. The peak represents n–$\pi^*$ to $\pi$–$\pi^*$ transition bands corresponding to a cross-linking reaction (Figure S3).[30] Similarly, the peak height at 350 nm was substantially increased between 5 and 12 min.

The increase of the peak height was fit to a logistic curve, which follows an autocatalytic reaction model

$$Y = \frac{Y_M \times Y_0}{(Y_M - Y_0)\, e^{-kt} + Y_0} \tag{2}$$

where $Y$ is peak intensity at a given time $t$, $Y_M$ and $Y_0$ are maximum and minimum peak intensity values, $k$ is the growth rate of nanoparticles or cross-links (Figure 2a-2).[31]

The number of nanoparticles formed in the gel was also controlled by the concentration of metal ionic precursors. Both the yellow color intensity and the height of UV absorption peak of the AgNP-hydrogel composites increased with the concentration of silver nitrate (Figure 2b).

Further incorporation of VP into the PEGDA hydrogel slowed down both the reduction rate of nanoparticles and the polymerization because the UV light at the wavelength of 253 nm, which was used for in situ gelation and particle polymerization, was likely absorbed by the PEGDA-PVP hydrogel (SI Figure S4). However, after completion of the reaction in 30 min, minimal difference of the number of AgNP was found between the PEGDA hydrogel and the PEGDA-PVP hydrogel.

**In Situ Nanoparticle Assembly Has Minimal Effect on the Stiffness of the AgNP-Hydrogel Composite.** This in situ assembly of the AgNP-hydrogel composite only minimally changed mechanical properties of the hydrogel. Elastic moduli of both AgNP-PEGDA hydrogel composite and pure PEGDA hydrogel were approximately 800 kPa (Figure 3a). Interestingly, the elastic modulus of the gel composite was independent of silver concentration in the pre-gelled mixture. The swelling ratio of the gel was also independent of the silver nitrate concentration. The independence of elastic modulus and swelling ratio on the silver concentration was also observed with the PEGDA–PVP hydrogel (Figure 3c).


DOI: 10.1021/acsami.5b03313
ACS Appl. Mater. Interfaces 2015, 7, 15359–15367

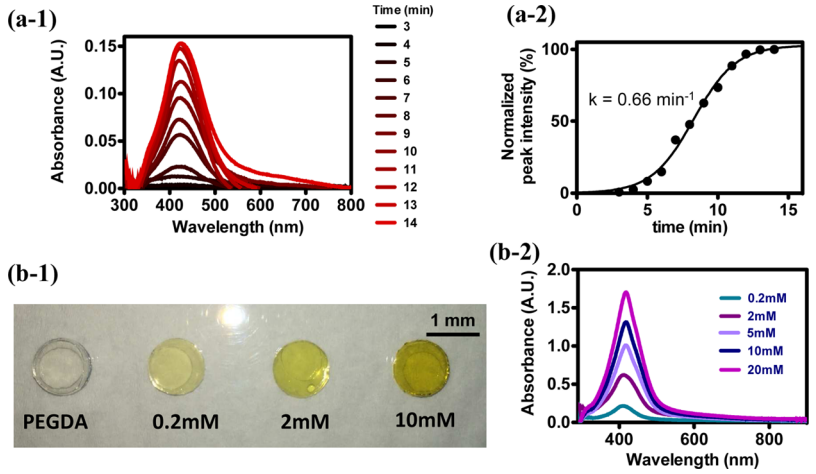


**Figure 2.** Analysis of in situ AgNP formation kinetics in the hydrogel. (a-1) UV/vis absorption spectra of AgNP formed by exposure of the aqueous mixture of 0.2 mM silver nitrate and PEGDA to UV light. (a-2) Increase of the absorbance intensity of AgNP at wavelength of 420 nm with the irradiation time. Data points were normalized by the feature rescaling method and fit to the sigmoidal fitting. (b-1) Optical images of the AgNP-PEGDA hydrogel composite prepared with varied concentrations of $AgNO_3$. (b-2) UV/vis absorption spectra of the AgNP-PEGDA hydrogel composite prepared with varied concentrations of silver nitrate. The spectra were acquired after UV irradiation of pre-gelled mixture over 10 min.

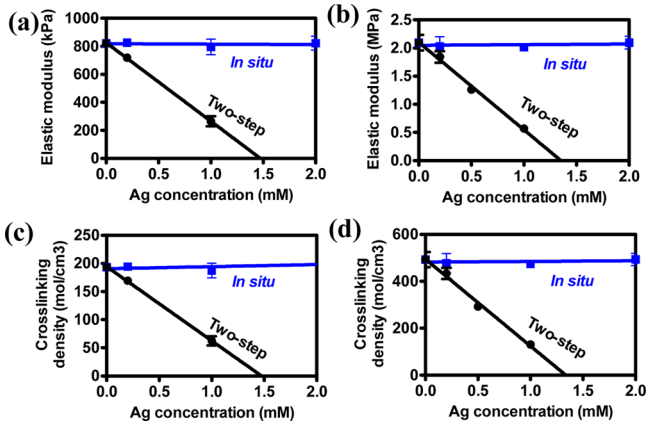


**Figure 3.** Analysis of physical properties and cross-linking density of the AgNP-PEGDA hydrogel composites. (a) Elastic moduli of the PEGDA hydrogel composites laden with controlled amount of AgNP prepared by either ″in situ″ assembly or "two-step" assembly. The "in situ" assembly was conducted by exposing the aqueous mixture of metallic salts and gel-forming polymer. The "two-step" assembly was conducted by incorporating prefabricated AgNP into a PEGDA solution followed by cross-linking reaction. (b) Elastic moduli of the AgNP-PEGDA-PVP hydrogel composite prepared by either "in situ" assembly or "two-step" assembly. (c) Cross-linking density of the AgNP-PEGDA hydrogel composites and (d) AgNP-PEGDA-PVP hydrogel composites prepared by either "in situ" assembly or "two-step" assembly. Data points and error bars represent average values and standard deviation of 3 different samples.

In contrast, the control condition, which was prepared by mixing premade AgNP with pre-gelled solution followed by activation of cross-linking reaction of PEGDA, displayed the linear decrease of an elastic modulus with silver precursor concentration (Figure 3a). Ultimately, the PEGDA solution mixed with premade AgNP at concentrations higher than 2 mM failed to form the gel. The inverse dependency of the elastic modulus on silver nitrate concentration was also observed with the PEGDA−PVP hydrogel composite.

Overall, according to the number of cross-links in the gel calculated using an elastic network model (see eq 5 in the Experimental Section), in situ gel composite assembly minimally influenced the cross-linked structure of the gel, while the premade nanoparticles substantially reduced the number of cross-links between polymers (Figure 3d). The same results were also found with the PEGDA-PVP hydrogel system (Figure 3e).

**Analysis of Nanoparticle Retention in the Hydrogels.** The gel composite prepared by the in situ assembly displayed enhanced retention of nanoparticles as compared with the two-step process in which premade nanoparticles were added into the PEGDA solution followed by activation of cross-linking reaction. Interestingly, during incubation of the in situ gel composites in DI water over 5 days, the concentration of AgNP in the PEGDA gel, calculated with the UV absorbance, decreased by 5% (Figure 4a). During the same period, the hydrogel composite prepared by the two-step process released more than half of the AgNP.

The gel's capability to retain nanoparticles was evaluated by measuring contents of AgNP and silver ions in incubation media using the inductively coupled plasma-mass spectroscopy (ICP-MS). The gel composite prepared via in situ assembly exhibited much smaller releases of AgNP and ions than that prepared by the two-step process (Figure 4b). The release rates ($\beta$) of AgNP and ions were further quantified using a first-order kinetic approximation (eq 3)

$$\frac{M_t}{M_\infty} = 1 - e^{-\beta t} \tag{3}$$

where $M_t$ and $M_\infty$ are the cumulative amounts of particles or ions released at time $t$ and at an infinite time, respectively. The gel composite prepared via in situ assembly displayed 15- and 3-fold lower $\beta$ values for AgNP and $Ag^+$ ions, respectively, compared with the composite prepared via the two-step process.

More interestingly, addition of VP into the AgNP-PEGDA gel composite system further reduced both released amounts and rates of AgNP and $Ag^+$ ions. Specifically, few AgNP were released from the PEGDA-PVP hydrogel prepared by the in situ assembly (Figure 4b-1). The $\beta$ value of $Ag^+$ ions was also 10-fold smaller than that for the gel composite prepared by the two-step process (Figure 4b-2).

**Antibacterial Activity of the AgNP-Hydrogel Composite.** The ability of the AgNP-hydrogel composite to control bacterial growth was evaluated by measuring bacterial growth


DOI: 10.1021/acsami.5b03313
ACS Appl. Mater. Interfaces 2015, 7, 15359−15367

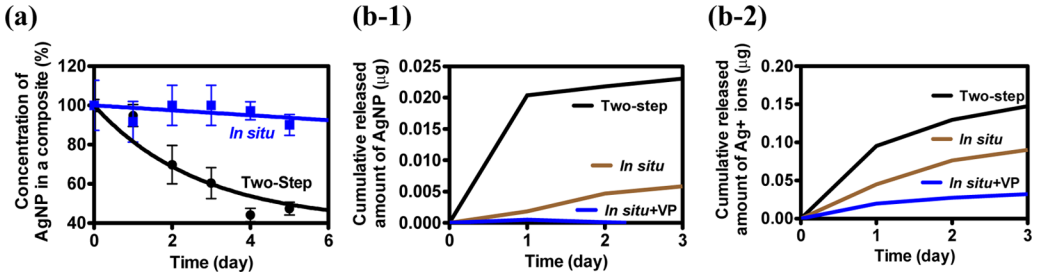


**Figure 4.** Analysis of capabilities of the PEGDA and PEGDA-PVP hydrogels to retain metallic nanoparticles and ions in the hydrogel. (a) Changes of the AgNP concentrations in a hydrogel prepared by either "in situ" assembly or "two-step" assembly. The nanoparticle concentrations were calculated from the UV/vis absorbance at the wavelength of 420 nm. (b) Accumulated ICP quantification of AgNP (b-1) and Ag+ ions (b-2) released from the hydrogel composites. In (b-1) and (b-2), "In situ+VP" indicates that the AgNP-PEGDA-PVP hydrogel composite prepared by the in situ assembly.

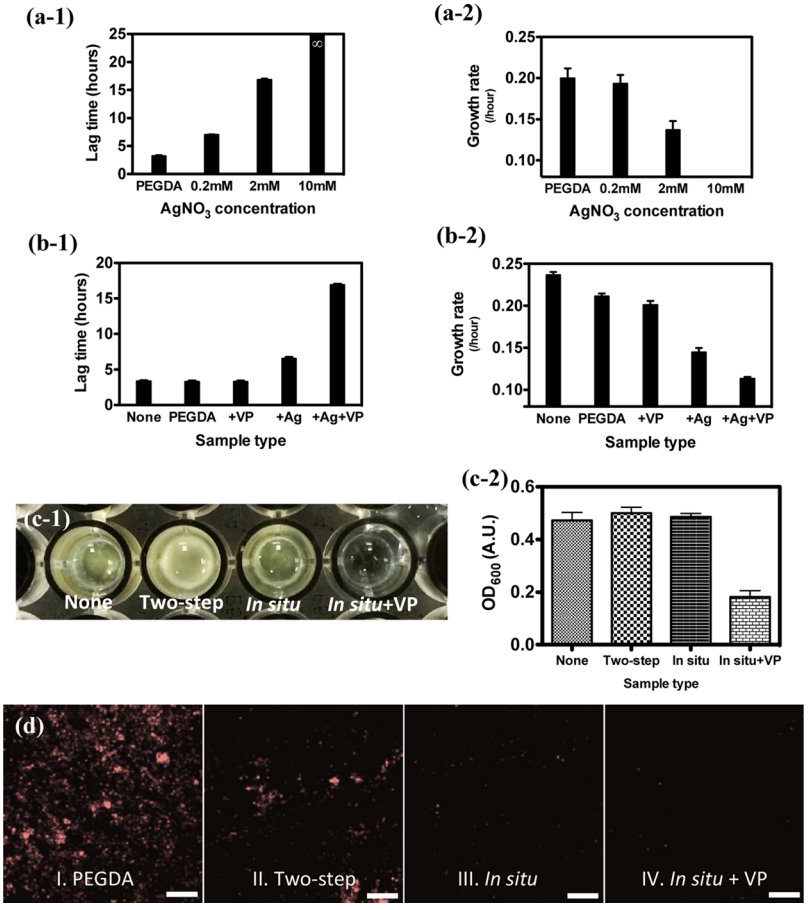


**Figure 5.** Antimicrobial activities of the AgNP-hydrogel composites against *E. coli* strains. (a) Lag time ($L_g$) (a-1) and growth rate ($G_R$) (a-2) of cells, challenged with gel composites prepared with different silver nitrate concentrations. (b) Lag time (b-1) and growth rate (b-2) of cells challenged with gel composites with different compositions. In (b-1) and (b-2), "None" represents the cell suspension not exposed to any gel composites, "PEGDA" represents that incubated with the pure PEGDA gel, "+VP" represents that incubated with the pure PEGDA−PVP hydrogel, "+Ag" represents that incubated with the AgNP-PEGDA gel composite, and "+Ag+VP" represents that incubated with the AgNP-PEGDA-PVP gel. All gels were prepared via the in situ assembly. In (a) and (b), *E. coli* cells suspended in the broth media were challenged with hydrogel composites while shaking the plate. (c) Evaluation of the long-term antibacterial activity of the hydrogel composites. Hydrogel composites were incubated for 10 days in DI water before adding them into the cell suspension. (c-1) Optic images of *E. coli* cell suspension challenged by the gel composites over 24 h. "Two step" and "In situ" represent the AgNP-PEGDA hydrogel composites prepared by the two-step and in situ assembly with 0.2 mM silver nitrate, respectively. (c-2) Absorbance intensity of cell suspension measured at wavelength of 600 nm. (d) Fluorescence images of the hydrogel surface exposed to the tdTomato fluorecence-expressing *E. coli*. In (d), "PEGDA" represents pure PEGDA hydrogel. "Two step" and "In situ" represent the AgNP-PEGDA hydrogel composites prepared by the two-step and in situ assembly with 0.2 mM silver nitrate, respectively. "In situ + VP" represent the AgNP-PEGDA-PVP hydrogel composites prepared by in situ photoactivated cross-linking reaction. The images were captured after incubation over 7 days. Scale bars represent 100 $\mu$m.

rates in media immersed with the composite. The AgNP-gel composites were immersed in the lysogeny broth (LB) media suspended with Gram-negative bacteria *Escherichia coli* at a density of $1.5 \times 10^6$ CFU/mL. Without the gel composite, the cell number analyzed with the optical density at 600 nm increased to $10^9$ CFU/mL within 8 h (SI Figure S5-a). The cell


DOI: 10.1021/acsami.5b03313
ACS Appl. Mater. Interfaces 2015, 7, 15359−15367

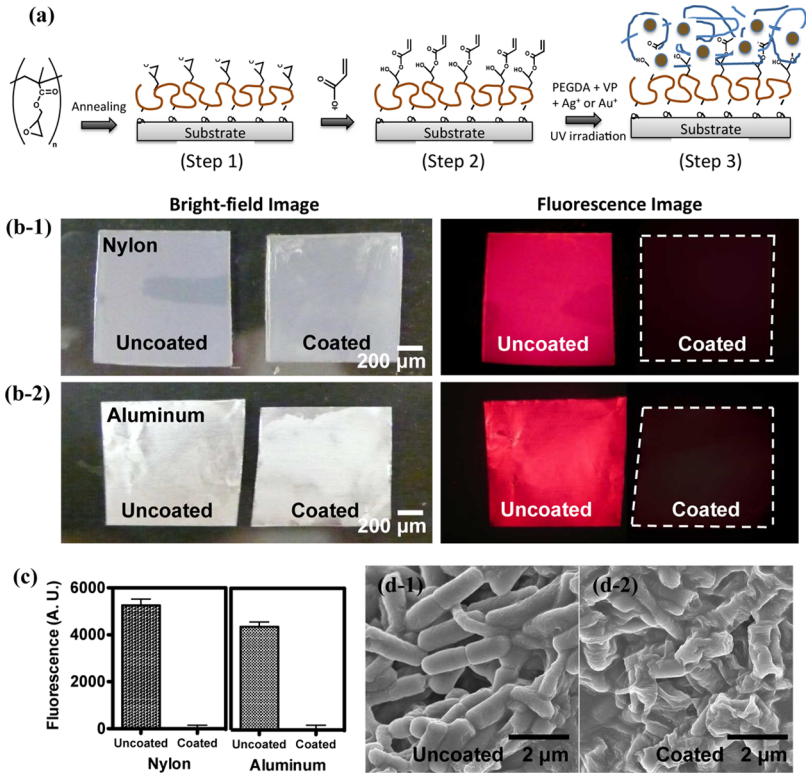


**Figure 6.** Mitigation of biofilm formation on nylon and aluminum substrates using the AgNP-PEGDA-PVP hydrogel composite as a coating material. (a) Scheme depicting sequential surface activation of target substrates (step 1) followed by immobilization of the AgNP-PEGDA-PVP hydrogel composite. (b) Optic (left) and fluorescence (right) images of tdTomato fluorescence from the uncoated and coated substrates. Images in (b-1) represent the nylon substrate and those in (b-2) the aluminum substrate. (c) Quantification of the fluorescence yield from the nylon and aluminum substrates either uncoated or coated by the AgNP-PEGDA-PVP hydrogel composites. (d) SEM images of bacteria collected from the nylon surface either uncoated or coated by the gel composites.

growth rate ($G_R$) was quantified by fitting the curve of optical density over time to a modified Gompertz growth model (eq 4)

$$Z = Z_0 + Z_M \exp\left\{-\exp\left[\left(\frac{eG_R}{Z_M}\right) \times (L_g - t) + 1\right]\right\} \quad (4)$$

where $Z$ is the viable cell count (log CFU/mL), $Z_0$ is the initial log number of cells, $Z_M$ is the difference between the initial and final cell numbers, $L_g$ is the lag time before the cell growth, and $t$ is the sampling time.[32]

The AgNP-PEGDA gel composite immersed into the cell media significantly influenced both $L_g$ and $G_R$. Increasing the initial silver concentration in the gel composite from 0 to 10 mM exponentially increased $L_g$ (Figure 5a-1). $G_R$ was also decreased with increasing silver concentration (Figure 5a-2). In particular, the PEGDA gel composite loaded with 10 mM silver, inhibited bacterial growth over 5 days.

More interestingly, the AgNP-PEGDA-PVP gel composite further limited the bacterial growth even at the silver concentration of 0.2 mM (Figure 5b-1). The $L_g$ was approximately 16 h, which was comparable to that attained with the 2 mM AgNP-PEGDA hydrogel composite. The $L_g$ was also about 3-fold longer than the 0.2 mM AgNP-PEGDA gel composite. The $G_R$ was also significantly decreased with the addition of VP into the gel composite (Figure 5b-2). In contrast, the pure PEGDA-PVP hydrogel (with no silver nanoparticles) had minimal influence on both $L_g$ and $G_R$.

Additionally, gel composites incubated in DI water over 10 days were challenged with fully saturated *E. coli* ($10^9$ CFU/mL), in order to assess the long-term antibacterial activities of the gel composites. Only AgNP-PEGDA-PVP hydrogel composites prepared by the in situ assembly lysed the bacterial cells by 80% and ultimately made the opaque bacterial cell suspension clear (Figure 5c).

The assembly method and composition of the gel composite also orchestrated to control biofilm formation on the gel surface (Figure 5d). As characterized by the tdTomato fluorescence-expressing *E. coli*, the pure PEGDA hydrogel allowed active bacterial cell adhesion and growth on its surface during incubation at 37 °C over 7 days (Figure 5d-I). The AgNP-PEGDA gel composite prepared by the two-step process significantly decreased the number of fluorescent *E. coli* on the gel; however, a certain number of bacterial cells adhered to the gel surface and underwent growth (Figure 5d-II). In contrast, both the AgNP-PEGDA gel composite and AgNP-PEGDA-PVP gel composite prepared by in situ assembly inhibited cell adhesion and growth (Figure 5d-III and IV) entirely.

**Evaluation of the AgNP-Hydrogel Composite as an Antibacterial Coating Material.** The resulting AgNP-PEGDA-PVP hydrogel composite was used as an antibacterial/antifouling coating material for various substrates including nylon and aluminum foil (Figure 6a). A thin, AgNP-hydrogel composite layer could be prepared by first coating substrates with poly(glycidyl methacrylate) (PGMA) and then spraying pre-gelled mixture followed by UV irradiation (Figure 6a).[33] The coated nylon and aluminum substrates largely prevented adhesion of bacterial cells when they were challenged with the fully saturated ($10^9$ CFU/mL) tdTomato fluorescence-express-


DOI: 10.1021/acsami.5b03313
ACS Appl. Mater. Interfaces 2015, 7, 15359−15367

ing *E. coli* at 37 °C over 10 days (Figure 6b,c). In contrast, uncoated substrates displayed strong red fluorescence from metabolically active bacterial cells. According to electron microscopic images of *E. coli* collected from the incubation media, cells incubated with uncoated substrates kept their cell membrane intact (Figure 6d-1 and SI Figure S6a). In contrast, cells incubated with the coated substrates were mostly punctured and lysed (Figure 6d-2 and SI Figure S6b).

**Discussion.** Taken together, this study successfully demonstrated that photoactivated, in situ AgNP and PEGDA-PVP gel assembly is advantageous in fabricating a hydrogel composite with sustained antifouling/antibacterial activities. We suggest that the in situ method is more effective than the two-step method, because there is minimal gel softening, less dispersal of nanoparticles, and a lower concentration of metallic nanoparticles is needed.

In the two-step composite process, gel softening caused by loading of prefabricated nanoparticles in the pre-gel solution is attributed to the limited cross-linking reaction between gel-forming polymers, particularly on the nanoparticle surface. It is highly likely nanoparticles with an average diameter of 9 nm sterically interfered with the cross-linking reaction between gel-forming polymers. Accordingly, the resulting gel would present a reduced number of interconnected polymeric networks responsible for the elastic response. As the number of defects is increased with nanoparticle concentration, the gel becomes softer proportionally to the number of particles loaded into the gel. In addition, uncontrolled aggregation between nanoparticles in the pre-gelled mixture would also contribute to the gel softening. In contrast, in situ nanoparticle assembly should not affect the cross-linking reaction, because the silver salts dissolved in the pre-gelled solution have equivalent size to the gel-forming polymer. Therefore, the resulting number of cross-links should be independent of AgNP concentration, thus leading to minimal change of gel stiffness. The stable binding between AgNP and the gel matrix may be an additional factor for the gel composite to undergo minimal softening. In addition, this in situ, one-step assembly allows us to avoid using reducing agents for nanoparticle synthesis. There is a possibility that the reducing agents remain in a gel matrix and negatively impact the environment and human health.[34] To the best of our knowledge, such nanoparticle-induced matrix softening has been neither addressed nor resolved to date.

Furthermore, this study demonstrated that the resulting AgNP-PEGDA-PVP hydrogel composite could be used as an antibacterial material to inhibit bacterial growth in a media as well as biofilm formation on material surfaces using a significantly smaller dose of AgNP than that used in past studies. These results were achieved by the enhanced binding between AgNP and the gel matrix, as confirmed with minimal release of nanoparticles and ions from the gel matrix. We suggest that the improved nanoparticle and ion retention in the gel is caused by coordination between tertiary amides of PVP and silver ions.[25] Previous studies adopted PVP in the AgNP synthesis, because of its capability to stabilize AgNP formation as a capping molecule.[25,26] We therefore suggest that the VP introduced into a pregelled solution stably associate with Ag ion and subsequently immobilize AgNP to the gel network via in situ cross-linking reaction. In contrast, the two-step process in which premade AgNP is introduced into the pre-gelled solution followed by cross-linking reaction should not be able to create the stable bonding between the matrix and AgNP, thus leading to the faster release of AgNP. Therefore, the AgNP and ions retained in the in situ fabricated gel composite could effectively damage the membrane of bacterial cells exposed to the gel surface. The underlying mechanism should be further systematically examined in future studies, because this is the first time the importance of a sustained presence of silver ions in a matrix for enhanced antibacterial control has been demonstrated. In the past, certain studies reported that a material designed to rapidly release silver ions is more favorable in controlling bacterial cell growth in aqueous media.[35]

## 3. CONCLUSION

In conclusion, this study demonstrated an advanced method to assemble the AgNP-PEGDA-PVP hydrogel composite that is structurally durable and also controls bacterial adhesion and contamination with a reduced amount of AgNP. The independence of the composite stiffness and the nanoparticle concentration, attained by the in situ assembly, was attributed to the balanced growth of nanoparticles and cross-linking reaction of polymers. The superior antibacterial activity of the gel composite was attributed to the sustained presence of AgNP and $Ag^+$ ions in the gel matrix, likely due to the coordination between AgNPs and PVP of the gel matrix. As such, polymeric and metallic substrates coated by the gel composite successfully inhibit biofilm formation on the surfaces. Overall, the AgNP-PEGDA-PVP gel composite developed in this study has the potential to take the quality of antibacterial control to a next level, with reduced concerns on the use of AgNP. Additionally, the results of this study may help improve the ratio of performance to particle loading for a wide array of metallic nanoparticle-laden polymer composite systems.

## 4. EXPERIMENTAL SECTION

**In Situ Assembly of AgNP-Hydrogel Composites.** The pre-gelled mixture was prepared by dissolving PEGDA (MW 1000 g/mol, Polysciences Inc.), vinylpyrollidone (VP, Sigma-Aldrich), Irgacure 2959 (0.1%, Ciba-Geigy), and silver nitrate. Concentrations of PEGDA and VP were kept constant at 20% and 10%, respectively. Concentrations of silver were varied from 0.2 to 10 mM. The pre-gelled mixture was placed between two glass plates separated by a spacer with 1 mm thickness. Then, the mixture was exposed to UV light (Jelight Co. Model 20, maximum UV wavelength 254 nm) for 10 min. The distance between the pre-gelled mixture and the UV lamp was kept constant at 1 cm. The resulting AgNP-hydrogel composites were cut into 5-mm-diameter disks for further analysis.

**Transmission Electron Microscope (TEM) Analysis of AgNP-Hydrogel Composites.** The hydrogel samples were fixed in Karnovsky's Fixative in phosphate buffered 2% glutaraldeyde and 2.5% paraformaldehyde and then washed in phosphate buffer saline solution. The samples were dehydrated in a series of increasing concentrations of ethanol. Acetonitrile was used as the transition fluid between ethanol and the epoxy. Infiltration series was done with an epoxy mixture using the Epon substitute Lx112. The resulting blocks were polymerized at 75 °C overnight, trimmed, and ultrathin sectioned with diamond knives. Sections were examined with a TEM (Jeol 2100), at 200 kV acceleration voltage.

**Analysis of Mechanical Properties of the Hydrogel Composites.** The elastic modulus of the gel composite was measured by uniaxially compressing the samples at a rate of 1 mm per minute using a mechanical testing system (MTS Insight). The slope of the stress versus strain curve was used to calculate


DOI: 10.1021/acsami.5b03313
ACS Appl. Mater. Interfaces 2015, 7, 15359−15367

the elastic modulus from the first 10% of strain. The number of cross-links ($N$) in the gel was calculated from the degree of swelling and elastic modulus using an elastic network model

$$N = \frac{SQ^{-1/3}}{RT} \quad (5)$$

where $S$ is the shear modulus calculated from the slope of the $\sigma$ versus $(\lambda - \lambda^{-2})$ curve assuming that the hydrogel follows an affined network model ($\sigma$: stress, $\lambda$: strain), $Q$ is the degree of swelling, $R$ is the gas constant (8.314 J mol$^{-1}$ K$^{-1}$) and $T$ is the temperature at which the $S$ and $Q$ were measured.[36]

**Inductively Coupled Plasma-Mass Spectroscopy (ICP-MS) Analysis.** To measure the total concentration of nanoparticles formed in hydrogels, a 0.5 cm$^3$ sample of composites was prepared and rinsed three times for 12 h. Then, AgNP-hydrogel composites were incubated in 2% ammonium persulfate solution to bleach out metallic nanoparticles in the gel. The silver concentration of the collected solution was measured using the ICP-MS (PerkinElmer - SCIEX ELAN DRCe). Separately, to measure release rates of AgNPs and $Ag^+$ ions, 0.5 mL sample of hydrogel composites was prepared, rinsed three times for 12 h, and incubated in centrifuge tubes with 6 mL of DI water at room temperature. One milliliter of supernatant was collected every 24 h and total amount of silver was analyzed by ICP-MS. Another 4 mL of supernatant was collected every 24 h. The nanoparticles were filtered through Amicon ultra centrifugal filter units (cut-off MW ~10 000 g/mol) by centrifugation. Then, silver ion content in the media was analyzed by the ICP-MS. The amount of released nanoparticles was calculated by subtracting the measured silver ion mass from the total silver mass.

**Analysis of Antibacterial Properties of AgNP-Hydrogel Composites.** Fresh *E. coli* (K12 TB1) was inoculated on an agar gel plate and incubated at 37 °C for a day, so the cells formed colonies. One colony was transferred to 5 mL of LB media in a tube using a sterile pipet tip. The tube was incubated at 250 rpm at 37 °C for 10 h. The bacterial suspension was diluted to 1.5 × 10$^8$ CFU/mL at which the optical density at wavelength of 600 nm ($OD_{600}$) became 1, and further diluted to 1.5 × 10$^6$ CFU/mL. Aliquots (20 $\mu$L) of hydrogel composites were added into 96 well plates, followed by loading 150 $\mu$L of dilute bacterial suspension. The absorbance at wavelength of 600 nm was measured for 24 h using a microplate reader (Tecan Infinite 200 PRO), while shaking the plate at 2 mm amplitude. The absorbance was used to quantify the lag time and the rate of bacterial growth. The assay was performed with four replicates for each sample.

**Preparation of *E. coli* Expressing tdTomato Fluorescence.** Competent *E. coli* were obtained using a mix-and-go *E. coli* transformation kit (Zymo Research) according to the manufacturer's recommendation. For transformation of cells, 1 ng of ptdTomato fluorescence plasmid DNA (Clontech Laboratories Inc.) was added to 50 $\mu$L of competent cells. The mixture was placed onto an agar-gel plate containing 100 $\mu$g/mL Ampicillin (Gold Biotechnology Inc.) and incubated at 37 °C. After 24 h, red-colored colonies appeared on the agar-gel plate.

**Analysis of Antibacterial Property of AgNP-Hydrogel Composites.** *E. coli* engineered to express tdTomato florescence was cultured in LB media supplemented with 100 $\mu$g/mL Ampicillin for 24 h before the experiment. AgNP-hydrogel composites with the size of 2 cm length × 2 cm width × 0.2 mm thickness were placed on the agar gel plate containing 100 $\mu$g/mL Ampicillin. 100 $\mu$L of engineered *E. coli* was placed on surface of the hydrogel composites. The plate was incubated at 37 °C for 7 days. After the incubation, the gel composites were detached from the agar gel. Then, cells attached to the gel composites were imaged using a laser scanning confocal microscope (Carl Zeiss LSM 700). The experiment was performed with 2 duplicates for each condition.

**Analysis of the Long-Term Antibacterial Property of the AgNP-Hydrogel Composites.** Twenty mm$^3$ of AgNP-hydrogel composites were incubated in DI water at room temperature for 10 days. DI water was replaced every day. The hydrogels were transferred to a 96 well plate. 150 $\mu$L of fully saturated *E. coli* suspension with 10$^9$ CFU/mL was added into each well. The plate was incubated at 37 °C without shaking, so cells readily sediment on gel surfaces. After 24 h, cells on the gel composites were imaged with an optical microscope. In parallel, $OD_{600}$ of the each well was measured with a plate reader. The experiment was performed with 4 duplicates for each condition.

**Coating of Nylon and Aluminum Substrates with AgNP-Hydrogel Composites.** First, poly(glycidyl methacrylate) (PGMA) was synthesized by radical polymerization of glycidyl methacrylate (GMA, 97%, Sigma-Aldrich). The mixture of 30% GMA and 1% of azobis(isobutyronitrile) (AIBN, 98%, Sigma-Aldrich) in methyl ethyl ketone (MEK) was stirred at 60 °C for 6 h. The synthesized PGMA was purified by repeated precipitation in diethyl ether, followed by drying in vacuum. Nylons and aluminum foils treated by plasma cleaner (Harrick Plasma PDC-32G) for 1 min were dip-coated in 1% PGMA dissolved in MEK, and subsequently annealed at 110 °C for 15 min. Next, the substrates were finally immersed in the acrylic acid to link PGMA with acrylic acid. Finally, a pregelled mixture of PEGDA and VP was placed on the surface of acrylic group-functionalized substrates followed by irradiation with UV light for 10 min. Then, the resulting substrates coated by the AgNP-hydrogel composites were washed with DI water to remove excess unreacted chemicals.

**Analysis of Antibacterial Properties of Substrates Coated by AgNP-Hydrogel Composites.** Both coated and uncoated substrates were placed in a 6-well plate. Three mL of fully saturated (10$^9$ CFU/mL) *E. coli* expressing tdTomato fluorescence was introduced into the well. The samples were incubated at 37 °C for 10 days. After the incubation, samples were gently rinsed with DI water 3 times and fluorescence from cells attached to the surface was visualized using a stereo fluorescence microscope (Nikon SMZ800). The fluorescence of substrates was measured using a plate reader (Tecan Infinite 200 PRO), in parallel. The substrates were excited at wavelength of 540 nm, and the subsequent emission yield at 581 nm was measured. The experiment was performed with 4 duplicates for each condition.

**Morphological Analysis of *E. coli* with a Scanning Electron Microscope (SEM).** The *E. coli* accumulated on substrates were collected by a sterile pipet tip and fixed in 4% formaldehyde solution. The cells were washed with DI water and centrifuged at 1000 rpm for 5 min. Then, the cells were dehydrated by repeatedly incubating them in an ethanol−water mixture with increasing ethanol concentrations (i.e., 35%, 50%, 75%, and 100%). Between each step, the samples were centrifuged at 3000 rpm for 5 min. The dehydrated cells were finally placed on a carbon tape and coated with platinum for charge dissipation. The morphologies of *E. coli* were observed using a scanning electron microscopy (Hitach 4800).


DOI: 10.1021/acsami.5b03313
ACS Appl. Mater. Interfaces 2015, 7, 15359−15367

## ■ ASSOCIATED CONTENT

### Supporting Information

Diffraction pattern of nanoparticles, nanoparticle aggregation in water, kinetics of PEGDA polymerization, UV/vis spectra of PEGDA-VP hydrogel, and raw data of bacteria growth in media. The Supporting Information is available free of charge on the ACS Publications website at DOI: 10.1021/acsami.5b03313.

## ■ AUTHOR INFORMATION

### Corresponding Authors

*E-mail: dhkim@kitech.re.kr.
*E-mail: hjkong06@illinois.edu.

### Notes

The authors declare no competing financial interest.

## ■ ACKNOWLEDGMENTS

This work was supported by Korea Institute of Industrial Technology (JE 140004 to D.H.K. and H.K.) and, partially, the National Institutes of Health (1R01 HL109192 to H.K.). TEM and SEM analysis were carried out in part in the Frederick Seitz Materials Research Laboratory Central Research Facilities, University of Illinois.

## ■ REFERENCES

(1) Costerton, J. W. Bacterial Biofilms: a Common Cause of Persistent Infections. *Science* **1999**, *284* (5418), 1318−1322.
(2) Hall-Stoodley, L.; Costerton, J. W.; Stoodley, P. Bacterial Biofilms: From the Natural Environment to Infectious Diseases. *Nat. Rev. Microbiol.* **2004**, *2* (2), 95−108.
(3) Flemming, H. C. Biofouling in Water Systems − Cases, Causes and Countermeasures. *Appl. Microbiol. Biotechnol.* **2002**, *59* (6), 629−640.
(4) Peleg, A. Y.; Hooper, D. C. Hospital-Acquired Infections Due to Gram-Negative Bacteria. *N. Engl. J. Med.* **2010**, *362* (19), 1804−1813.
(5) Bouillard, L.; Michel, O.; Dramaix, M.; Devleeschouwer, M. Bacterial Contamination of Indoor Air, Surfaces, and Settled Dust, and Related Dust Endotoxin Concentrations in Healthy Office Buildings. *Ann. Agric. Environ. Med.* **2005**, *12* (2), 187−192.
(6) D'Ercole, S.; Scarano, A.; Perrotti, V.; Mulatinho, J.; Piattelli, A.; Iezzi, G.; Tripodi, D. Implants with Internal Hexagon and Conical Implant-Abutment Connections: an in Vitro Study of the Bacterial Contamination. *J. Oral. Implantol.* **2014**, *40* (1), 30−34.
(7) Dizaj, S. M.; Lotfipour, F.; Barzegar-Jalali, M.; Zarrintan, M. H.; Adibkia, K. Antimicrobial Activity of the Metals and Metal Oxide Nanoparticles. *Mater. Sci. Eng., C* **2014**, *44*, 278−284.
(8) de Faria, A. F.; de Moraes, A.; Marcato, P. D. Eco-Friendly Decoration of Graphene Oxide with Biogenic Silver Nanoparticles: Antibacterial and Antibiofilm Activity. *J. Nanopart. Res.* **2014**, *16*, 2110.
(9) Xiu, Z.-M.; Zhang, Q.-B.; Puppala, H. L.; Colvin, V. L.; Alvarez, P. J. J. Negligible Particle-Specific Antibacterial Activity of Silver Nanoparticles. *Nano Lett.* **2012**, *12* (8), 4271−4275.
(10) Hajipour, M. J.; Fromm, K. M.; Ashkarran, A. A.; de Aberasturi, D. J.; de Larramendi, I. R.; Rojo, T.; Serpooshan, V.; Parak, W. J.; Mahmoudi, M. Antibacterial Properties of Nanoparticles. *Trends Biotechnol.* **2012**, *30* (10), 499−511.
(11) Sondi, I.; Salopek-Sondi, B. Silver Nanoparticles as Antimicrobial Agent: a Case Study on E. Coli as a Model for Gram-Negative Bacteria. *J. Colloid Interface Sci.* **2004**, *275* (1), 177−182.
(12) Rai, M.; Yadav, A.; Gade, A. Silver Nanoparticles as a New Generation of Antimicrobials. *Biotechnol. Adv.* **2009**, *27* (1), 76−83.
(13) Sharma, V. K.; Yngard, R. A.; Lin, Y. Silver Nanoparticles: Green Synthesis and Their Antimicrobial Activities. *Adv. Colloid Interface Sci.* **2009**, *145* (1−2), 83−96.
(14) Leawhiran, N.; Pavasant, P.; Soontornvipart, K.; Supaphol, P. Gamma Irradiation Synthesis and Characterization of AgNP/Gelatin/PVA Hydrogels for Antibacterial Wound Dressings. *J. Appl. Polym. Sci.* **2014**, *131* (23), 41138.
(15) González-Sánchez, M. I.; Perni, S.; Tommasi, G.; Morris, N. G.; Hawkins, K.; López-Cabarcos, E.; Prokopovich, P. Silver Nanoparticle Based Antibacterial Methacrylate Hydrogels Potential for Bone Graft Applications. *Mater. Sci. Eng., C* **2015**, *50*, 332−340.
(16) Vimala, K.; Kanny, K.; Varaprasad, K.; Kumar, N. M.; Reddy, G. S. M. Novel-Porous-Ag0 Nanocomposite Hydrogels via Green Process for Advanced Antibacterial Applications. *J. Biomed. Mater. Res.* **2014**, *102* (12), 4616−4624.
(17) Fullenkamp, D. E.; Rivera, J. G.; Gong, Y.-K.; Lau, K. H. A.; He, L.; Varshney, R.; Messersmith, P. B. Mussel-Inspired Silver-Releasing Antibacterial Hydrogels. *Biomaterials* **2012**, *33* (15), 3783−3791.
(18) Mohan, Y. M.; Lee, K.; Premkumar, T.; Geckeler, K. E. Hydrogel Networks as Nanoreactors: a Novel Approach to Silver Nanoparticles for Antibacterial Applications. *Polymer* **2007**, *48* (1), 158−164.
(19) Thoniyot, P.; Tan, M. J.; Karim, A. A.; Young, D. J.; Loh, X. J. Nanoparticle−Hydrogel Composites: Concept, Design, and Applications of These Promising, Multi-Functional Materials. *Adv. Sci.* **2015**, *2*, No. 10.1002/advs.201400010.
(20) Badr, Y.; Mahmoud, M. A. Manifestation of the Silver Nanoparticles Incorporated Into the Poly Vinyl Alcohol Matrices. *J. Mater. Sci.* **2006**, *41* (12), 3947−3953.
(21) Thomas, V.; Yallapu, M. M.; Sreedhar, B.; Bajpai, S. K. A Versatile Strategy to Fabricate Hydrogel−Silver Nanocomposites and Investigation of Their Antimicrobial Activity. *J. Colloid Interface Sci.* **2007**, *315* (1), 389−395.
(22) Murthy, P. S. K.; Murali Mohan, Y.; Varaprasad, K.; Sreedhar, B.; Mohana Raju, K. First Successful Design of Semi-IPN Hydrogel−Silver Nanocomposites: a Facile Approach for Antibacterial Application. *J. Colloid Interface Sci.* **2008**, *318* (2), 217−224.
(23) Yu, H.; Xu, X.; Chen, X.; Lu, T.; Zhang, P.; Jing, X. Preparation and Antibacterial Effects of PVA-PVP Hydrogels Containing Silver Nanoparticles. *J. Appl. Polym. Sci.* **2006**, *103* (1), 125−133.
(24) Reidy, B.; Haase, A.; Luch, A.; Dawson, K.; Lynch, I. Mechanisms of Silver Nanoparticle Release, Transformation and Toxicity: a Critical Review of Current Knowledge and Recommendations for Future Studies and Applications. *Materials* **2013**, *6* (6), 2295−2350.
(25) Wang, H.; Qiao, X.; Chen, J.; Wang, X.; Ding, S. Mechanisms of PVP in the Preparation of Silver Nanoparticles Mater. *Chem. Phys.* **2005**, *94* (2−3), 449−453.
(26) Tejamaya, M.; Römer, I.; Merrifield, R. C.; Lead, J. R. Stability of Citrate, PVP, and PEG Coated Silver Nanoparticles in Ecotoxicology Media. *Environ. Sci. Technol.* **2012**, *46* (13), 7011−7017.
(27) Maretti, L.; Billone, P.; Liu, Y.; Scaiano, J. Facile Photochemical Synthesis and Characterization of Highly Fluorescent Silver Nanoparticles. *J. Am. Chem. Soc.* **2009**, *131* (39), 13972−13980.
(28) McGilvray, K. L.; Decan, M. R.; Wang, D.; Scaiano, J. C. Facile Photochemical Synthesis of Unprotected Aqueous Gold Nanoparticles. *J. Am. Chem. Soc.* **2006**, *128* (50), 15980−15981.
(29) Ingle, J. D. J.; Crouch, S. R. *Spectrochemical Analysis*; Prentice Hall, 1988.
(30) González-Henríquez, C. M.; del C Pizarro, G.; Sarabia-Vallejos, M. A.; Terraza, C. A.; López-Cabaña, Z. E. In Situ-Preparation and Characterization of Silver- HEMA/PEGDA Hydrogel Matrix Nanocomposites: Silver Inclusion Studies Into Hydrogel Matrix. *Arab. J. Chem.* **2014**, 1−11.
(31) Reed, L. J.; Berkson, J. The Application of the Logistic Function to Experimental Data. *J. Phys. Chem.* **1929**, *33* (5), 760−779.
(32) Zwietering, M. H.; Jongenburger, I.; Rombouts, F. M.; van 't Riet, K. Modeling of the Bacterial Growth Curve. *Appl. Environ. Microbiol.* **1990**, *56* (6), 1875−1881.
(33) Liu, Y.; Klep, V.; Zdyrko, B.; Luzinov, I. Polymer Grafting via ATRP Initiated From Macroinitiator Synthesized on Surface. *Langmuir* **2004**, *20* (16), 6710−6718.
(34) Mulfinger, L.; Solomon, S. D.; Bahadory, M.; Jeyarajasingam, A. V.; Rutkowsky, S. A.; Boritz, C. Synthesis and Study of Silver Nanoparticles. *J. Chem. Educ.* **2007**, *84* (2), 322.
(35) Hetrick, E. M.; Schoenfisch, M. H. Reducing Implant-Related Infections: Active Release Strategies. *Chem. Soc. Rev.* **2006**, *35* (9), 780.


DOI: 10.1021/acsami.5b03313
*ACS Appl. Mater. Interfaces* 2015, 7, 15359−15367

(36) Anseth, K. S.; Bowman, C. N.; Brannon-Peppas, L. Mechanical Properties of Hydrogels and Their Experimental Determination. *Biomaterials* **1996**, *17* (17), 1647−1657.



DOI: 10.1021/acsami.5b03313
*ACS Appl. Mater. Interfaces* 2015, 7, 15359−15367